Sixth International Symposium on Turbulence and Shear Flow Phenomena
Seoul, Korea, 22-24 June 2009

LARGE-EDDY SIMULATION OF WEAKLY COMPRESSIBLE FLOW AROUND AIRFOIL — MODELING THE SOUND SOURCE —

Takeo Kajishima
Department of Mechanical Engineering,
Osaka University
2-1 Yamadaoka, Suita, Osaka, 565-0871, Japan
kajisima@mech.eng.osaka-u.ac.jp

Masayuki Kiyono
Department of Mechanical Engineering,
Osaka University
2-1 Yamadaoka, Suita, Osaka, 565-0871, Japan
kiyono@fluid.mech.eng.osaka-u.ac.jp

Takeshi Omori
Department of Mechanical Engineering,
Osaka University
2-1 Yamadaoka, Suita, Osaka, 565-0871, Japan
t.omori@mech.eng.osaka-u.ac.jp

ABSTRACT

The objective of our research is to improve the prediction of aerodynamic performance and particularly noise generation. To this end, we offer an efficient method to deal with compressible turbulent flow around a body at low Mach number. This paper deals with the low-Mach number flow around NACA0012 airfoil. Particular attention is focused on the effect of compressibility on the unsteady phenomena in the vicinity of the solid boundary. The pressure equation, which is the partial differential equation of elliptic type, is modified to account for weak compressibility. In LES, we applied a one-equation dynamic model for subgrid scale turbulence. In our result for Reynolds number 2×10^5 and Mach number 0.06, the velocity divergence is visible in the region near the leading edge, where Powell's model indicates the sound source. Our results suggested that the weakly compressible method in conjunction with LES can directly capture the sound source in the flow at low-Mach numbers.

INTRODUCTION

The analysis of aerodynamic noise around objects moving at high Reynolds number and low Mach number is a hopeful subject of CFD development. Examples include flows around a high-speed train, an airplane at takeoff and a large scale wind turbines.

Existing approaches are categorized into the direct method and the separated method. In the direct method, the sound source is provided as a result of DNS (Direct Numerical Simulation) of Navier-Stokes equation of compressible fluid flow. The direct method must deal with wide range of scale in space and time. In addition, the strength of sound pressure is much smaller than the pressure fluctuation of flow. The direct method is therefore difficult for a practical tool.

In the separated method, the unsteady flow is solved by the incompressible scheme and the acoustic field is calculated by using the approximated sound source given by the flow simulation. LES (Large Eddy Simulation) may be one of an appropriate way for generating the sound source model in high-Reynolds number flows. As for the sound source, theoretical methods have been proposed by Curle (1955), Powell (1964) or Howe (2003) on the basis of acoustic analogy of Lighthill (1952).

Our strategy is included in the separated method, but we intend to improve the sound source model. Namely, LES in couple with a weakly compressible scheme is used to obtain the density fluctuation around the solid object in the low Mach number flow.

We developed an efficient scheme for low Mach number flow and integrated into the LES to deal with high Reynolds number flow. The one-equation dynamic model by Kajishima and Nomachi (2006) is used for the SGS (Subgrid scale) model. The present method can provide the information of density fluctuation with small amount of additional computation in comparison with the incompressible scheme. Since the pressure is solved by an elliptic partial-differential equation, a distinct merit of our method is suitability for flow of Mach number ranging from zero to approximately 0.3. Typical example is the rotating blade of the MW class wind turbine.

In this paper, first, our numerical result of LES around NACA0012 airfoil is compared with available experimental data by Miyazawa et al. (2003, 2004). Then the divergence of velocity field is compared with a theoretical model of sound source to discuss the possibility of new concept for the analysis of aerodynamic noise.

OUTLINE OF COMPUTATION

Flow field of low Mach number is usually simulated by the incompressible flow scheme due to the severe limitation of time-increment in the compressible flow scheme. In this work, we propose a modification in the usual incompress-

ible scheme, based on the elliptic equation for pressure, to improve the accuracy for turbulent flows considering weak compressibility.

Basic Equations for LES

The filtered equations of mass and momentum conservation of compressible fluid is represented by

$$\frac{\partial \bar{\rho}}{\partial t} + \frac{\partial (\bar{\rho}\tilde{u}_j)}{\partial x_j} = 0, \tag{1}$$

$$\frac{\partial (\bar{\rho}\tilde{u}_j)}{\partial t} + \frac{\partial (\bar{\rho}\tilde{u}_i\tilde{u}_j)}{\partial x_j} = -\frac{\partial}{\partial x_i}(\bar{p} + \frac{2}{3}\bar{\rho}k_S) + \frac{\partial \sigma_{ij}}{\partial x_j}, \tag{2}$$

where $\bar{(\ )}$ denotes filtering and $\tilde{(\ )}$ is the Favre mean. The eddy viscosity assumption is applied for residual stress, which is usually interpreted as an SGS stress. ρ, p and u_i are density, pressure and velocity. In the equation of perfect gas

$$\bar{p} = \bar{\rho}RT, \tag{3}$$

we assume the isothermal field. The molecular viscosity μ is also assumed constant. In Eq. (2),

$$\sigma_{ij} = 2(\mu + \mu_S)(\bar{D}_{ij} - \frac{1}{3}\delta_{ij}\bar{D}_{kk}) \tag{4}$$

is the stress tensor, where $\bar{D}_{ij}$ is deformation rate tensor.

SGS model

At this stage, the compressibility is not taken into account for the SGS stress for simplicity. We introduced a dynamic procedure into the one-equation SGS model (Okamoto and Shima, 1999). In our model (Kajishima and Nomachi, 2006), the energy production term in the transport equation of SGS kinetic energy k_S is dynamically determined. The SGS eddy viscosity μ_S is represented as

$$\mu_S = C_\nu \Delta_\nu \bar{\rho}\sqrt{k_S} \tag{5}$$

by using $k_S = \tau_{ii}/(2\bar{\rho})$, where $\tau_{ij} = \bar{\rho}(\widetilde{u_i u_j} - \tilde{u}_i\tilde{u}_j)$. k_S is calculated by the transport equation.

Our one-equation dynamic SGS model applies the dynamic procedure for the energy transfer. Namely, in the production term in the k_S transport equation

$$\frac{\partial k_S}{\partial t} + \frac{\partial (k_S\tilde{u}_j)}{\partial x_j} = -\tau^a_{ij}\bar{D}_{ij} - C_\varepsilon\frac{k_S^{3/2}}{\bar{\Delta}} - \varepsilon_\omega + \frac{\partial}{\partial x_j}[(C_d\Delta_\nu\sqrt{k_S} + \nu)\frac{\partial k_S}{\partial x_j}], \tag{6}$$

τ^a_{ij} is determined by the dynamic Smagorinsky model, where the superscript a denotes the anisotropic part. As for the characteristic length Δ_ν,

$$\Delta_\nu = \frac{\bar{\Delta}}{1 + C_k\bar{\Delta}^2|\bar{D}|^2/k_S} \tag{7}$$

is used to represent the behavior in the vicinity of the solid wall. The dissipation term is modified by addition of

$$\varepsilon_\omega = 2\nu\frac{\partial\sqrt{k_S}}{\partial x_j}\frac{\partial\sqrt{k_S}}{\partial x_j}. \tag{8}$$

The merit of using k_S is that the boundary condition of $\tau_{ij} = 0$ is automatically satisfied by the boundary condition $k_S = 0$. Moreover, in our method, any artificial correction such as the van Driest dumping or spatial averaging is not necessary.

Time Marching Method

The time marching of the Navier-Stokes equation of motion is divided into 2 steps by the fractional step method:

$$\frac{(\rho\boldsymbol{u})^F - (\rho\boldsymbol{u})^n}{\Delta t} = \nabla\cdot\{-(\rho\boldsymbol{u}\boldsymbol{u}) + \tau\}, \tag{9}$$

$$\frac{(\rho\boldsymbol{u})^{n+1} - (\rho\boldsymbol{u})^F}{\Delta t} = -\nabla p^{n+1} \tag{10}$$

where $t_n = n\Delta t$ and Δt is the time increment. $\boldsymbol{\tau}$ is the viscous stress. Any appropriate explicit scheme can be used for the right-hand side of Eq.(9). In our simulation, the second-order Adams-Bashforth is applied. For the spatial difference, the second-order central finite-difference is used, except for QUICK scheme for the convection term.

In between Eqs.(9) and (10), one should solve p^{n+1}. Coupling the mass conservation equation

$$\frac{\rho^{n+1} - \rho^n}{\Delta t} + \nabla\cdot(\rho\boldsymbol{u})^{n+1} = 0 \tag{11}$$

with Eq.(10) derives the elliptic equation for p^{n+1}. To eliminate ρ^{n+1}, considering the small change of Δp and $\Delta\rho$ in one time step, we use the approximated equation of state

$$p^{n+1} - p^n = (\rho^{n+1} - \rho^n)RT \tag{12}$$

where T is assumed to be constant. Thus the pressure equation is represented by

$$\nabla^2 p^{n+1} - \frac{p^{n+1}}{RT(\Delta t)^2} = \frac{\nabla\cdot(\rho\boldsymbol{u})^F}{\Delta t} - \frac{p^n}{RT(\Delta t)^2}. \tag{13}$$

The effect of compressibility is represented by the second term of each side. In our simulation, Eq.(13) is solved by SOR method.

Bondary Conditions

To remove the unphysical reflection of pressure wave at the inflow and outflow boundaries, we used the method developed by Okita and Kajishima (2002). We use the transport equation for pressure

$$\frac{\partial p}{\partial t} + U_m\left[\frac{\partial p}{\partial x}\right]^I + (U_m + \frac{1}{M})\left[\frac{\partial p}{\partial x}\right]^C = 0, \tag{14}$$

where x is the direction of main flow and U_m is the convective speed at the boundary. The superscript I means the incompressible component and C is the compressible component.

The I portion in Eq.(14) is related to the convective condition considering the consistency to the Navier-Stokes equation (2)

$$\left[\frac{\partial p}{\partial x}\right]^I = -(u_j - \bar{U}_j)\frac{\partial(\rho u_j)}{\partial x_j} \tag{15}$$

On the other hand, the C portion is given by

$$\left[\frac{\partial p}{\partial x}\right]^C = \frac{\partial p}{\partial x} - \left[\frac{\partial p}{\partial x}\right]^I. \tag{16}$$

RESULTS AND DISCUSSION

The compressibility affects the accuracy of flow prediction even in a low Mach number. Moreover, the capturing of small density fluctuation is important in the study of aerodynamic noise. In this study, we conducted 3-dimensional LES (Large-Eddy Simulation) of flow around a 2-dimensional NACA0012 airfoil. As the Mach number is low, the flow field is usually treated as incompressible. In this section, the result by weak-compressibility method is compared with that by the incompressible method. Moreover, the one-equation dynamic model is compared with the standard Smagorinsky model. Then the property of leading-edge separation and related density fluctuation are analyzed.

Computational Conditions

The setup is corresponding to the experiment by Miyazawa and Kato (2003): the angle of attack, 9°; the velocity of uniform stream, $U_0 = 20.0$m/s; the chord length, $C = 0.15$m. The Reynolds number is 2×10^5. Mach number is estimated as 5.76×10^{-2}.

The coordinate is selected as x in the mainstream direction, z in the span-wise direction and y in the direction perpendicular to x and z. In x-y plane, the body-fitted computational grid of 'C' type is used. In z direction, the uniform space grid is used with the periodic boundary condition. The size of domain is: the diameter of a half circle of 'C' grid is $8C$; $8C$ in the wake side; $2C$ in the span-wise direction. The numbers of grid point are: 1600 in the circumferential, and 800 on the blade surface; 160 to the outward from the surface; 128 in the span-wise direction. The minimum of the grid width is: $5.35 \times 10^{-4}C$ in the circumferential, $2.31 \times 10^{-4}C$ normal to the surface.

The initial condition is a uniform flow. After the marching of non-dimensional time 16, the statistics of the flow field is obtained. The averaged flow field shown hereafter is the average in 3 non-dimensional time as well as in the span-wise direction.

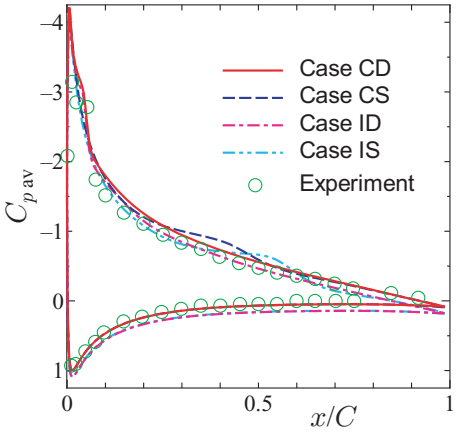

(a) time-averaged pressure coefficient

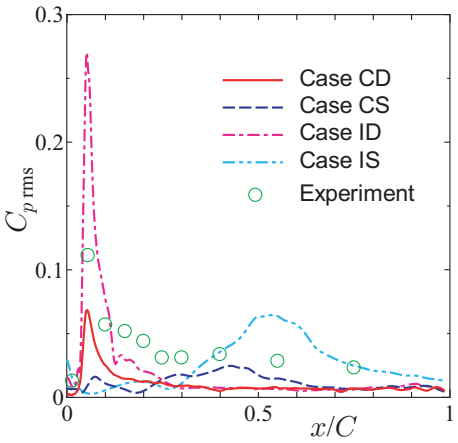

(b) intensity of fluctuation on suction side

Figure 1: Pressure coefficient on the surface

Flow Field

The positions of separation and re-attachment along the chord are estimated at $0.018C$ and $0.058C$, respectively. In the experiment by Miyazawa, et al. (2003), they observed the laminar separation bubble in the similar region. As shown in an instantaneous flow field of Fig.??, unsteady vortices are captured by our simulation and they are thought to be a sound source (Miyazawa, et al., 2003, 2004).

Since the Mach number is very low, the density fluctuation is lower than 1% in Case CD. Low density regions are observed in the cores of vortices in separated region. The experimental result suggested the existence of extensive sound source in this region.

In the experiment, there seems high intensity in broad range, with two peaks at around 1800Hz and 3600Hz, in the spectrum of pressure fluctuation on the wall near the leading edge. In our result, the frequency of the vortices in this region is estimated to be in 3300∼4000Hz. Thus it can be concluded that our method, which consists of (1) weakly compressible scheme, (2) one-equation dynamic SGS model and (3) usage of velocity divergence for sound source, is promising as a new methodology of aero-acoustics.

Fig.1(a) shows the time-averaged pressure coefficient $C_{p\,\mathrm{av}}$ on the airfoil surface. Fig.1(b) shows the pressure fluctuation $C_{p\ \mathrm{rms}}$, without contribution of SGS component, on the suction side. Cases CD, CS, ID and IS denote the weak compressibility with one-equation dynamic model, the weak compressibility with Smagorinsky model, the incompressibility with one-equation dynamic model, and the incompressibility with Smagorinsky model, respectively. Smagorinsky model could not reproduce the flow separation near the leading edge and pressure fluctuation due to the separation, which were measured by the experiment. The model overestimated pressure fluctuation in the chord center on the suction surface. On the other hand, the one-equation model could reproduce the flow separation. But the pressure fluctuation was overestimated especially in the incompressible method. Note that the intensity of filtered fluctuation should be lower than that of raw data. The result by case CD, namely the one-equation dynamic model taking into account the weak compressibility, showed reasonable result.

In the experiment (Miyazawa, et al., 2003, 2004) the laminar separation in the region near the leading edge of the suction side and the laminar flow on the pressure side were observed. Smagorinsky model gives SGS eddy viscosity even in the region where GS component is not turbulent. This is thought to be the reason that the separation bubble was not reproduced as shown in Fig.1(a). On the other hand, our one-equation dynamic model gave reasonable result.

Sound Source

Figure 2 shows an instantaneous distribution of sound source given by the Powell's model (19xx) in the x-y cross section. This is given by $\nabla \cdot (\boldsymbol{\omega} \times \boldsymbol{u})$ and approximates vortex sound source. As shown in Fig. 2, there are elongated

patterns near the leading edge in the suction side. They indicate alternate positive-negative regions. Fig. 3, on the other hand, shows the profile of $\nabla \cdot \boldsymbol{u}$ for the same instance and cross-section to Fig. 2. This value is related to $D\rho/Dt$ and it therefore is interpreted as a phenomenon related to the sound source. Actually, similar patterns are observed in the region close to the leading edge in Figs. 2 and 3. In the turbulent boundary layer after the re-attachment, there seems some disturbance in Fig. 2 but they do not have significant fluctuation of the density as shown in Fig. 3.

Figure 4 shows an instantaneous profile of the span-wise component of vorticity ω_z in x-y plane near the leading edge. Fig. 5 shows a close-up view of $\nabla \cdot \boldsymbol{u}$ (shown in Fig. 3) at the section corresponding to Fig. 4. In the region of unsteady vortices, quadruple patterns of $\nabla \cdot \boldsymbol{u}$ are observed near the core of unsteady ω_z.

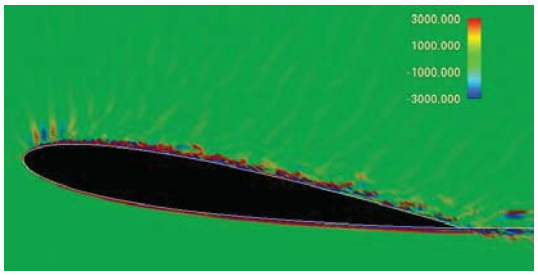

Figure 2: Instantaneous distribution of Powell's sound source around the airfoil

Figure 3: Instantaneous distribution of $\nabla \cdot \boldsymbol{u}$ around the airfoil

CONCLUSION

An efficient numerical method suited for weakly compressible flow was proposed. Then it was applied to LES of flow around a NACA0012 airfoil at low Mach number. The pressure profile due to the separation bubble was successfully reproduced by LES in comparison with experiment. Based on the LES database, we estimated the source of aerodynamic noise. The velocity divergence $\nabla \cdot \boldsymbol{u}$ was confirmed to be corresponding to the Powell's model for sound source. It suggested that our combination method of weakly compressible scheme and one-equation dynamic SGS model is promising for representing the sound source from the flow at low Mach number.

REFERENCES

Curle, N., 1955, "The influence of solid boundaries upon aerodynamic sound", *Proc. R. Soc.*, Vol. A231, pp. 505-514.

Howe, M. S., 2003, "Theory of vortex sound", Cambridge University Press.

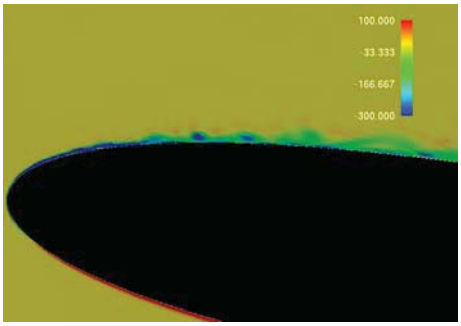

Figure 4: Instantaneous distribution of vorticity ω_z near the leading edge

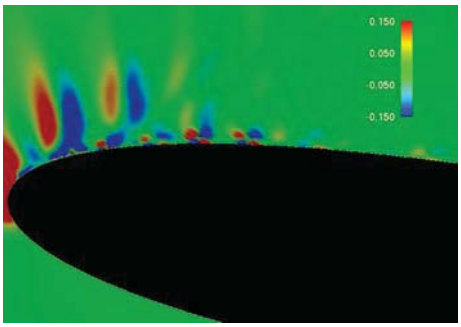

Figure 5: Instantaneous distribution of $\nabla \cdot \boldsymbol{u}$ near the leading edge

Kajishima, T. and Nomachi, T., 2006, "One-equation subgrid scale model using dynamic procedure for the energy production" *Trans ASME Journal of Applied Mechanics*, Vol.73, Issue 3, pp.368-373.

Lighthill, M. J., 1952, "On sound generated aerodynamically 1. General theory", *Proc. R. Soc.*, Vol. A211, pp. 564-587.

Okamoto, M., and Shima, N., 1999, "Investigation for the one-equation-type subgrid model with eddy-viscosity expression including the shear-dumping effect," *JSME Int. J., Ser. B*, Vol.42, No.2, pp.154-161.

Okita, K. and Kajishima, T., 2002, "Numerical simulation of unsteady cavitating flows around a hydrofoil", *Trans JSME, Ser.B*, Vol. 68, No. 667, pp. 637-644 (in Japanese).

Powell, A., 1964, "Theory of vortex sound", *J. Acoust. Soc. Am.*, Vol. 36, pp. 177-195.

Miyazawa, S., et al., 2003, *Proc. 18th NST Symposium*, pp. 66-61 (in Japanese).

Miyazawa, S., et al., 2004, *Proc. 18th Symposium on Computational Fluid Dynamics*, No. B1-2 (in Japanese).